1 Snow cover variations across China from 1951-2018

2 **Xiaodong Huang[1*], Changyu Liu[2], Zhaojun Zheng[3], Yunlong Wang[2], Xubing Li[1], and**
3 **Tiangang Liang[2]**

4 [1] School of Geographical Sciences, Nanjing University of Information Science and Technology, Nanjing
5 210044, China
6 [2] State Key Laboratory of Grassland Agro-ecosystems, College of Pastoral Agriculture Science and
7 Technology, Lanzhou University, Lanzhou, 730020, China
8 [3] Key Laboratory of Radiometric Calibration and Validation for Environmental Satellites, National
9 Satellite Meteorological Center, China Meteorological Administration, Beijing, 100081, China
10 *Correspondence to*: Xiaodong Huang (huangxd@lzu.edu.cn)

11

12 **Abstract.** Based on a snow depth dataset retrieved from meteorological stations, this experiment
13 explored snow indices, including snow depth (SD), snow covered days (SCDs), and snow phenology
14 variations, across China from 1951 to 2018. The results indicated that the snow cover trends across China
15 exhibits regional differences. The annual mean SD tended to increase, and the increases in mean and
16 maximum snow depth were 0.04 cm and 0.1 cm per decade, respectively. SCDs tended to increase by
17 approximately 0.5 days per decade. The significant increases were concentrated at latitudes higher than
18 40°N, especially in Northeast China. However, in the Tibetan Plateau, the SD and SCDs tended to
19 decrease but not significantly. Regarding the snow phenology variations, the snow duration days in China
20 decreased, and 25.2% of the meteorological stations showed significant decreasing trends. This result
21 was mainly caused by the postponement of the snow onset date and the advancement of the snow end
22 date. Geographical and meteorological factors are closely related to snow cover, especially the change in
23 temperature, which will lead to significant changes in snow depth and phenology.
24 Keywords: Snow; Ground observations; Change; China

25 **1   Introduction**

26 Snow covers 40% of the global land surface in winter, and more than 90% of seasonal snow cover is
27 concentrated in the Northern Hemisphere (Armstrong and Brodzik, 2001), stretching across an area of
28 approximately 4.6×10^7 km^2. Snow cover represents an essential component of the energy exchange
29 process and hydrological cycle within the global climate system (Euskirchen et al. 2007; Yao et al. 2013).
30 Snow cover has a unique physical attribute of high albedo (Xiao and Che, 2016), which has a positive
31 feedback effect on climate (Tedesco and Miller, 2007). Within the global hydrological cycle, snow cover
32 not only affects the water cycle but also constitutes a highly crucial form of water storage (Ambadan,
33 2017; Shams et al., 2018). However, snow can also have negative impacts on human life because snowfall
34 and meltwater are direct causes of snowmelt erosion, snowmelt floods, avalanches, and other natural
35 disasters (Li & Simonovic, 2010; Chen et al., 2016).

36   As an essential climate variable, snow cover has received much attention around the world, and various
37 snow datasets can be used to evaluate snow cover variations. Currently, the Rutgers University Global
38 Snow Lab and the binary snow cover mask data derived from the Climate Data Record of the Northern
39 Hemisphere Snow Cover Extent (NHSCE) can provide a long-term snow dataset (1967-present).
40 However, the dataset is appropriate for only large-scale snow extent studies because of the coarse spatial
41 resolution (24 km), much coarser for the 1967-1998 portion of the record (190.5 km resolution) (Brown
42 & Robinson, 2011). In addition, the implementation of the interactive multi-sensor snow and ice mapping
43 system (IMS) provides another approach for the dynamic monitoring of snow extent (Sönmez et al. 2014).

1 Other sensors with moderate resolution, such as Moderate Resolution Imaging Spectroradiometer
2 (MODIS), can provide global snow extent products with high resolution and accuracy, but the record
3 period is short (2000 to present) (Hall et al., 2002). Passive microwave remote sensing has been regarded
4 as an efficient way to retrieve snow depth (SD) or snow water equivalent (SWE) data at hemisphere and
5 global scales, such as the Scanning Multichannel Microwave Radiometer (SMMR), Special Sensor
6 Microwave/Imager (SSM/I), and Advanced Microwave Scanning Radiometer-EOS (AMSR-E). Another
7 technique that assimilates in situ snow depth observations with microwave emissions was applied in the
8 European Space Agency's (ESA) GlobSnow project to estimate the daily SWE time series from 1979 to
9 present over the Northern Hemisphere (GlobSnow v3.0 SWE CDR released in 2019), and this technique
10 is considered to overcome the large errors that rely solely on passive microwave observations (Pulliainen
11 et al. 2006; 2020; Takala et al., 2011). However, while the GlobSnow SWE algorithm exhibits improved
12 accuracy, the data gaps in alpine areas limit its comprehensive use in snow variation assessments.

13 Early satellite observations in the Northern Hemisphere suggested a decline in the snow cover extent
14 (SCE) over the past several decades, even though the spatial trend patterns are variable between different
15 observations. The SCE has experienced a well-documented decrease in spring, and arguably, there has
16 been a slight increase or decrease in winter (the statistical significance of the linear trend is very weak)
17 in satellite observations since the late 1980s in the Northern Hemisphere (Brown and Robinson, 2011;
18 Choi et al, 2010; Cohen et al. 2014; Connolly et al. 2019; Mudryk et al. 2020). The pattern of the remote
19 sensing observations is quite different from the Coupled Model Intercomparison Project Phase 5 (CMIP-
20 5) predictions, in which the CMIP5 models imply that SCE have steadily decreased for all seasons.
21 (Connolly et al. 2019). The spring SCE that was determined using the NHSCE between 1967 and 2012
22 over the Northern Hemisphere was compared with the CMIP-5 model output, which revealed that the
23 reductions in the spring SCE from 2008–2012 exceeded the CMIP-5 projections (Derksen and Brown,
24 2012). Multi-dataset analysis shows decrease in SCE in all months from 1981 to 2014 in Northern
25 Hemisphere, and the CMIP-6 multi-model ensemble better represents the snow extent climatology for
26 all months, correcting a low bias in CMIP-5 (Mudryk et al. 2020). During the period from 2000 to 2015,
27 the SCE in high-latitude and high-elevation mountainous regions decreased significantly, while the SCE
28 at some middle and low latitudes showed increasing trends in the Northern Hemisphere (Wang et al.,
29 2018). In Eurasia, the SCE decreased significantly only in June, and there is no obvious trend of SCE in
30 winter from 2000 to 2016 (Sun et al. 2020). A delayed snow onset date was observed to be the main
31 driver of decreasing annual snow duration trends, and the spatial pattern of annual snow duration trends
32 exhibited noticeable asymmetry between continents, with the largest significant decreases observed over
33 western Eurasia with relatively few statistically significant decreases over North America (Hori et al.,
34 2017). This finding shows the regional differences from the hemispheric average trends for the Northern
35 Hemisphere (Brown & Robinson, 2011; Wang et al., 2018; Connolly et al., 2019). In contrast to SCE,
36 the annual mean SD decreased in most areas over North America (Dyer & Mote, 2006) and increased in
37 Eurasia and the Arctic (Kitaev et al., 2005; Liston & Hiemstra, 2011). Accordingly, the overall snow
38 mass trends were negative over North America, and for Eurasia, the trend was negligible for the
39 investigated non-alpine regions from 1980 to 2018 (Pulliainen et al., 2020).

40 Limited by the coarse spatial resolution, poor accuracy and short observation periods from remote
41 sensing data, in situ snow depth observations provide the most reliable dataset for analyzing the changes
42 in snow cover with a high degree of credibility. Moreover, snow parameters are calculated from
43 meteorological station data, which have great advantages in the process of long time series research.
44 Measurements of daily snow depth were conducted at 1103 meteorological stations over the Eurasian

1   continent from 1966 to 2012 to provide a detailed description of snow depth variability. These
2   measurements revealed that both the annual mean and the maximum SD showed increasing trends over
3   the entire Eurasian continent, including China, and the snow depth decreased in autumn and increased in
4   spring and winter (Zhong et al. 2018). Daily snow observation data from 672 stations in China during
5   the period from 1952–2010 were used to analyze snow cover days (SCDs) and snow cover phenology
6   variations (Ke et al. 2016). The results indicated that from 1952 to 2010, the overall snow phenology in
7   China reflected a delay of the snow onset date (SOD) and an advancement of the snow end date (SED).
8   The reduced temperature and increased mean air temperature were the main reasons for the overall late
9   snow onset and early snow end day.

10   In recent years, the variations in snow cover over China have attracted much attention, especially with
11   regard to the so-called 'third pole' of the Tibetan Plateau due to it being the region with the highest
12   elevation and deepest snow depth at middle latitudes in the Northern Hemisphere (Ma et al., 2010). A
13   previous study using remote sensing snow products indicated that the annual mean SCE accounts for 27%
14   of the country's total area in winter, and the average annual SCE decreased during winter and summer
15   but increased in spring and fall over the last 14 years; however, these trends were not statistically
16   significant (Huang et al., 2016). Driven by decreased temperature and increased precipitation in the snow
17   accumulation season, the snow cover fraction over mainland China showed an increasing trend of 0.29%
18   per decade during 1982–2013, which was significant at the 0.05 level (Chen et al. 2016). Overall, the
19   SCE varied slightly but did not increase or decrease significantly for the Chinese mainland. The SOD
20   moved forward slightly, but the SED has become significantly earlier at the rate of 1.91 days per decade,
21   with a 73% contribution from the decreased SCE between 1982 and 2013 in China (Chen et al., 2016).

22   SD is a basic and important parameter of snow cover that plays an important role in hydrological
23   applications, numerical weather predictions, climate change research and land surface process
24   simulations. However, reliable quantitative knowledge of long-term seasonal snow cover and its trend is
25   lacking. Therefore, we aim to explore the snow cover variations in China from 1951 to 2018 based on an
26   SD dataset retrieved from meteorological stations. The objectives are to 1) evaluate the spatial
27   distributions of various snow parameters, 2) ascertain the variation trends and fluctuation periods of those
28   snow parameters, 3) compare the trends of those snow parameters among the three stable snow cover
29   areas of China, and 4) analyze the spatiotemporal dynamics of snow heterogeneity by using geographical
30   and meteorological factors throughout China.

31   **2   Dataset and methodology**

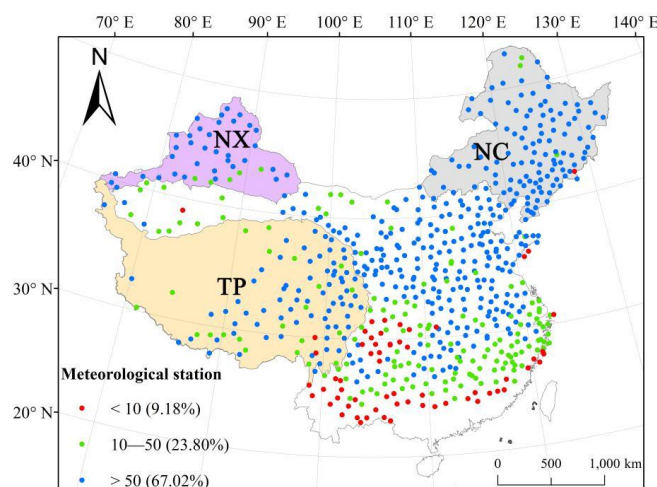32   **2.1   Snow depth records**

1 **Figure 1.** Geographical locations and the proportion of valid yearly records between 1951 and 2018 for
3 each meteorological station in mainland China. The abbreviations of snow cover areas represent the
4 Tibetan Plateau (TP), northern Xinjiang (NX), and Northeast China (NC).
5 Snow depth datasets were obtained from 730 meteorological stations from January 1, 1951, to December
6 31, 2018, in China, which were provided by the National Meteorological Information Center of the China
7 Meteorological Administration (CMA) (http://data.cma.cn/en). A hydrological year spanned from July 1
8 of the current year to June 30 of the subsequent year to capture the entire seasonal snow cycle. Therefore,
9 the data from July 1, 1951, to June 30, 2018, were used in this study, which include 67 seasonal snow
10 cycles in total (Figure 1). Snow depth of ground observations is measured manually with a wooden ruler
11 at 8 o'clock every day when the ground in the field of view around the meteorological station is covered
12 by more than half in snow. The measurements are made thrice and the distance between the three
13 measurements is more than 10 m. The measured value is accurate to 0.1 cm. The final snow depth at each
14 station was determined as the average of the three measurements, and an average snow depth of less than
15 0.5 cm is recorded as 0. Initially, the data quality control standards implemented in this study were as
16 follows. 1) Only daily SD values larger than 1 cm were recorded as snow cover; stations with SD values
17 less than 1 cm were regarded as snow free. 2) Stations with records spanning less than 10 years were
18 omitted from the analysis to ensure the reasonableness of the statistical analysis. Therefore, 67 stations
19 with snow records less than 10 years were omitted from the analysis in this study.
20   The snow cover parameters, including the annual mean snow depth (SD$_{overall}$), maximum snow depth
21 (SD$_{max}$), SCDs, SOD, SED, and snow duration days (SDDs), were calculated for each selected
22 meteorological station (Table 1). To avoid the impact of ephemeral snow in snow phenology
23 computations, SOD was defined as the first date of the first three continuous snow records, and SED was
24 defined as the last day of the date of last three continuous snow records (Chen et al. 2016; Ke et al. 2016).
25 The difference between the numbers of SCDs and SDDs is that SCDs include ephemeral snow days
26 beyond the snow season, which may be longer than SDDs.
27 **Table 1**. The abbreviations and descriptions of snow parameters

Abbreviation	Description
SD$_{overall}$	Calculated by dividing the sum of snow depth records by the total number of days in a hydrological year

SD$_{max}$	The maximum snow depth for the corresponding hydrologic year
SCDs	The total days characterized by snow-covered ground throughout a hydrological year
SOD	The first date of snow onset in the snow accumulation season during a hydrological year
SED	The snow end date during the snow melting season
SDDs	The number of days from the SOD to the SED in a corresponding hydrological year

1

2 **2.2 Meteorological data**

3 Meteorological data with a 1 km resolution were selected in this study. The dataset was provided by the
4 "Loess Plateau Data Center, National Earth System Science Data Sharing Infrastructure, National
5 Science & Technology Infrastructure of China (http://loess.geodata.cn)". The dataset time series is from
6 1901 to 2017. In this study, the annual mean temperature (Tmp-mean), annual total precipitation (Pre-
7 sum), annual maximum monthly precipitation (Pre-max), annual mean lowest temperature (Tmn-mean),
8 annual mean maximum temperature (Tmx-mean), annual coldest monthly minimum temperature (Tmn-
9 min), and annual warmest monthly maximum temperature (Tmx-max) from 1951 to 2017 in the dataset
10 were used to explore the heterogeneity of snow cover.

11 **3 Methodology**

12 **3.1 Trend analysis**

13 Linear fitting is the most common and extensive trend analysis method. Moreover, the Mann-Kendall
14 (M-K) test is also recommended by the World Meteorological Organization and is frequently used to
15 analyze the trends of changes in meteorological and hydrological elements (Milan, 2013). In this study,
16 these two methods were used to analyze the trends of the variations in the snow cover indices from 1952
17 to 2012. The M-K test formulas are as follows:

18 $S = \sum_{j=1}^{n-1} \sum_{i=j+1}^{n} sign(x_i - x_j)$ (1)

19 where n is the number of years to be analyzed. x_i and x_j are the values in time series i and j, respectively.

20
$$
\begin{cases}
Z = \dfrac{(S-1)}{\sqrt{\frac{n(n-1)(2n+5)}{18}}} & S > 0 \\
Z = 0 & S = 0 \\
Z = \dfrac{(S+1)}{\sqrt{\frac{n(n-1)(2n+5)}{18}}} & S < 0
\end{cases}
\qquad (2)
$$

21 where Z is the value used to judge whether the trend is increasing or decreasing in the trend analysis.
22 When Z is positive, the trend is increasing, while negative values of Z represent decreasing trends. At the
23 same time, by comparing the absolute value of Z with the standard value of Z, we can determine the
24 significance of the trend. In this study, significance levels of α=0.05 and α=0.01 are used. If the absolute
25 value of Z is greater than $Z_{0.05}$ or $Z_{0.01}$, the trend is statistically significant or extremely significant,
26 respectively.

27 $S_k = \sum_{i=1}^{k} r_i, r_i = \begin{cases} 1, x_i > x_j \\ 0, x_i \le x_j \end{cases}, (j = 1,2,\dots,i; k = 1,2,\dots,n)$ (3)

28 $E[S_k] = \dfrac{k(k-1)}{4}$ (4)

29 $var[S_k] = \dfrac{k(k-1)(2k-5)}{72} \quad 1 \le k \le n$ (5)

30 $UF_k = \dfrac{(S_k - E[S_k])}{\sqrt{var[S_k]}}$ (6)

The Cryosphere
Discussions

1   $UB_k = -UF'_k, UF'_k = UF_{n-k}$ (7)

2   where UF is the standardized value of S, while UF' is obtained by inverting the sequence of UF.

3   In the M-K test, when the UF is greater than 0, there is an increasing trend from the initial year to

4   the corresponding year; when the UF is less than 0, there is a decreasing trend. Similarly, when UB is

5   greater than 0, there is an increasing trend from the corresponding year to the end year, and when UB is

6   less than 0, there is a decreasing trend. UF and UB can provide the approximate break points of the

7   meteorological sequence. However, the break points of the meteorological sequence can be further

8   judged by combining the M-K and moving t tests. When t is greater than $t_{0.05}$, the year corresponding to

9   t represents a break point. The formulas for the moving t test are as follows:

10   $t = \dfrac{(\bar{x}_1 - \bar{x}_2)}{s\sqrt{\frac{1}{n_1}+\frac{1}{n_2}}}$ (8)

11   $s = \sqrt{\dfrac{n_1 s_1^2 + n_2 s_2^2}{n_1 + n_2 - 2}}$ (9)

12   In this study, the slope method is also employed to analyze the snow cover variation trend (Stow et al.

13   2004). The formula is as follows:

14   $slope = \dfrac{n\sum_{i=1}^{n} i x_i - \sum_{i=1}^{n} i \sum_{i=1}^{n} x_i}{n\sum_{i=1}^{n} i^2 - (\sum_{i=1}^{n} i)^2}$ (10)

15   where n is the number of datasets to be analyzed and x_i is the value in the time series i.

16   **3.2   Structural equation model**

17   Structural equation modeling (SEM) is a statistical method based on a variable covariance matrix

18   that can be used to analyze the relationships between variables (Bagozzi and Yi, 2012). This method

19   synthesizes a variety of statistical methods, including path analysis, regression analysis, and factor

20   analysis. Path analysis is a method to analyze the multilayer relationship and correlation intensity

21   between multiple variables. In this study, path analysis was employed to analyze the effect of

22   geographical and meteorological factors on the spatial and temporal heterogeneity of snow cover. To

23   avoid collinearity within the variables, a factor importance screening function was carried out for variable

24   selection. Finally, seven factors including altitude, latitude, longitude, Tmp-mean, Pre-sum, Tmx-max,

25   and Tmn-min were screened out. Conceptual models of the hypothesized relationships showing the direct

26   and indirect effects of geographical and meteorological variables on the snow parameters are shown in

27   Figure 2. The standardized path coefficients for SME assume that latitude, longitude and altitude directly

28   affect precipitation and temperature and thus indirectly affect snow cover, while precipitation and

29   temperature have a direct impact on snow cover. The maximum likelihood algorithm was used to estimate

30   the model parameters and determine the goodness-of-fit of the model (Grace et al., 2010). The model

31   output of the path coefficients are standardized regression coefficients. The total standardized effects

32   consist of direct and indirect standardized effects. High path coefficients indicate large effects of a

33   predictor variable on the response variable (Grace et al., 2016). The formula for the maximum likelihood

34   method is as follows:

35   $F_{ML} = \log|\Sigma(\theta)| + tr\left(S \sum(\theta)^{-1}\right) - \log|S| - (p+q)$ (11)

36   $S = \begin{pmatrix} var(y) & cor(y,x) \\ cor(x,y) & var(x) \end{pmatrix}$ (12)

37   $\Sigma(\theta) = \begin{pmatrix} var(x) + var(e) & var(x) \\ var(x) & var(x) \end{pmatrix}$ (13)

38   where the core of the maximum likelihood method is to minimize the function $F(S, \sum(\theta))$. S is the

39   sample covariance matrix, and $\sum(\theta)$ is the implicit covariance of the structural variable.

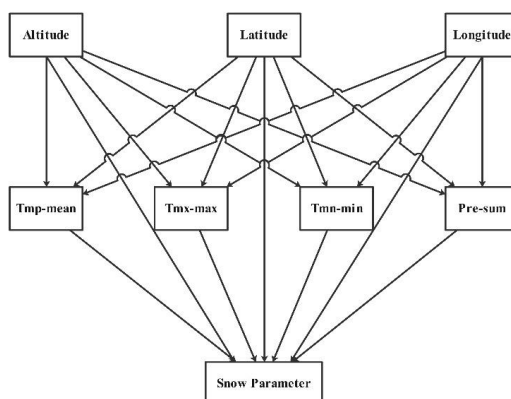The Cryosphere
Discussions
Open Access
EGU

1

2   **Figure 2.** Conceptual models of the hypothesized relationships showing the direct and indirect effects

3   of geographical and meteorological variables on snow parameters

4   **4   Results**

5   **4.1   SD**

6   The mean annual $SD_{overall}$ and SD_{max} gradually increase with increasing latitude and altitude in China

7   from 1951 to 2018 (Figure 3a and c). The largest mean $SD_{overall}$ of 9.3 cm is found in northern Xinjiang,

8   while the largest annual mean SD_{max} (55.3 cm) appears in the Tibetan Plateau. Overall, the mean $SD_{overall}$

9   and SD_{max} are 0.7 cm and 9.4 cm, respectively. $SD_{overall}$ and SD_{max} both tend to increase by 0.05 cm and

10   0.1 cm per decade from 1951 to 2018, respectively. Additionally, the distributions of the $SD_{overall}$ and

11   SD_{max} trends are similar (Figure 3b, and d). The stations in China with significant increases in $SD_{overall}$

12   and SD_{max} are concentrated mainly at high latitudes, and the proportions of meteorological stations with

13   significant increases in $SD_{overall}$ and SD_{max} are 9.8% and 7.3%, respectively. In contrast, the stations with

14   significant decreases in $SD_{overall}$ and SD_{max} are concentrated mainly in the Tibetan Plateau and central

15   China, and the proportions of meteorological stations with significant decreases in $SD_{overall}$ and SD_{max} are

16   7.1% and 5.6%, respectively. Table 2 also shows that the overall $SD_{overall}$ and SD_{max} tend to increase

17   significantly in Northeast China, increasing by 0.2 cm and 0.7 cm per decade, respectively. These values

18   in northern Xinjiang tend to increase but not significantly. In the Tibetan Plateau, however, $SD_{overall}$ and

19   SD_{max} both show decreasing trends, but the trends are negligible.

20   **Table 2** Trends in SD across the three snow cover areas of China from 1951 to 2018.

Zone	Variate	Slope analysis		M-K analysis
		Slope	P-value	Z-value
Northeast	$SD_{overall}$	0.02	0.00**	3.51**
	SD_{max}	0.07	0.00**	3.00**
Northern Xinjiang	$SD_{overall}$	0.01	0.15	1.22
	SD_{max}	0.04	0.14	1.68
Tibetan Plateau	$SD_{overall}$	-0.00	0.78	-0.13
	SD_{max}	-0.00	0.79	-0.02

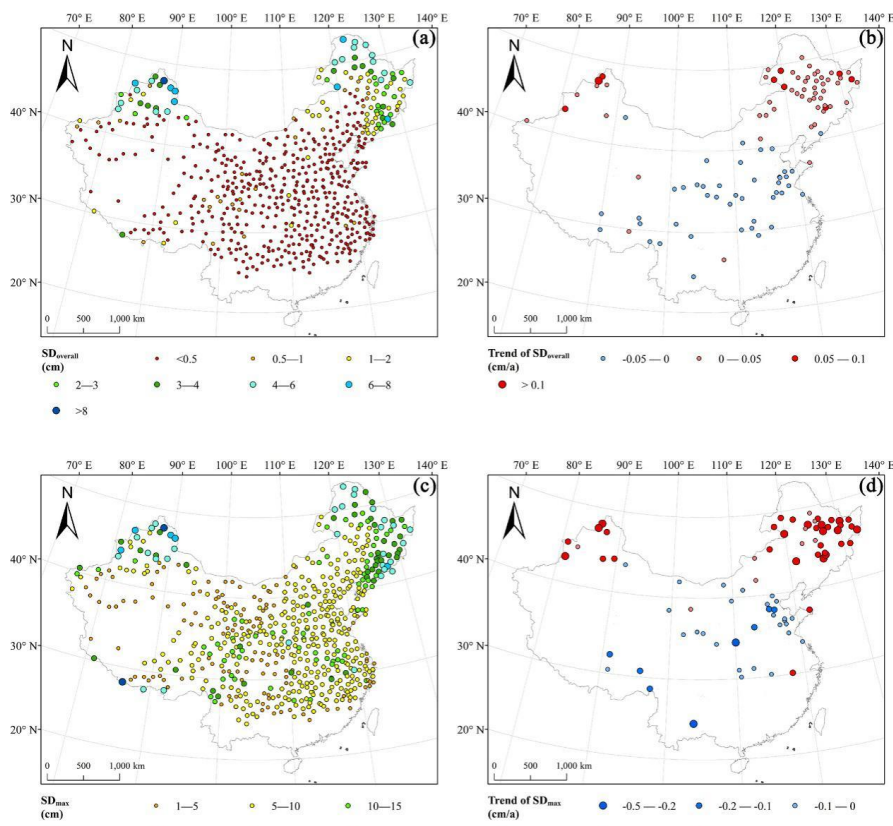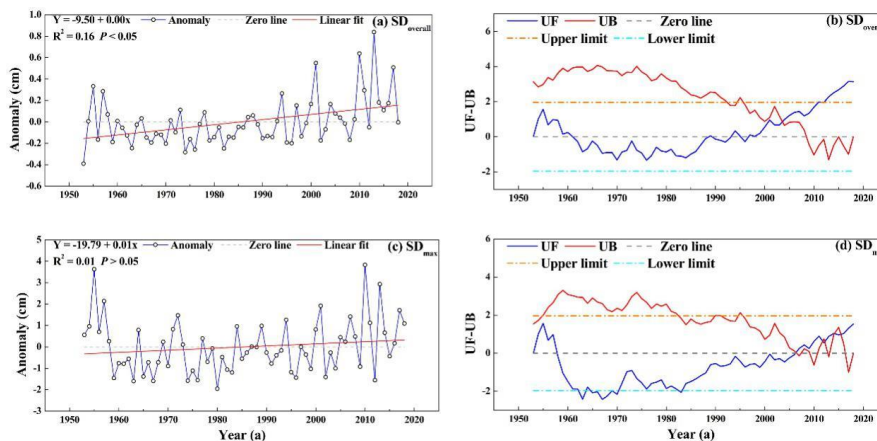21   ** denotes a significant change at $P < 0.05$.

22

1

2 **Figure 3.** Panels (a) and (c) represent the spatial distributions of the mean annual $SD_{overall}$ and the mean

3 SD_{max} across China, respectively, and panels (b) and (d) show the distributions of the trends of the mean

4 annual $SD_{overall}$ and the mean SD_{max}, respectively, as determined by the trend analysis to exhibit

5 significant changes ($P < 0.05$) across China.

6

7

1   **Figure 4.** Panels (a) and (c) present the linear fits of the mean annual $SD_{overall}$ and the mean SD_{max} across

2   China, respectively, and panels (b) and (d) present the results of the M-K test of the mean annual $SD_{overall}$

3   and the mean SD_{max} in China, respectively.

4   The results of the M-K trend test are the same as those of the slope method (Figure 4). In China, the

5   overall trends of $SD_{overall}$ and SD_{max} first increase, then decrease, and finally increase again during the

6   period from 1951 to 2018. The trend of $SD_{overall}$ changes in 1961 and 1997, whereas the SD_{max} trend

7   changes in 1958 and 2007. Table 3 shows that the break point of $SD_{overall}$ occurs in 2003; for SD_{max}, the

8   break point appears in 2006. In Northeast China, the $SD_{overall}$ break point occurs in 1999, while the SD_{max}

9   break point is observed in 2004. In northern Xinjiang, the $SD_{overall}$ break point appears in 2006, while the

10   SD_{max} break point occurs in 2000. In the Tibetan Plateau, the $SD_{overall}$ break point is observed in 1957,

11   and a break point of SD_{max} appears in 2004. In summary, except for the $SD_{overall}$ break point of the Tibetan

12   Plateau, which appears in 1957, the $SD_{overall}$ and SD_{max} break points of the three snow cover areas are all

13   in the vicinity of China and are concentrated between 1999 and 2006.

14   **Table 3.** Break points of snow cover index variations detected by a moving t test.

	$SD_{overall}$	SD_{max}	SCDs	SOD	SED	SDDs
China	2003	2006	1999	1959, 1964	2004	2005
Northeast	1999	2004	1999	2005	2001	2000
Northern Xinjiang	2006	2000	1993, 2002	1970	1996	1999，2001
Tibetan Plateau	1957	2004	—	2001	2009	2005

15

16   **4.2 SCDs**

17   The mean annual SCDs gradually increase with increasing latitude and altitude in China from 1951 to

18   2018 (Figure 5a), and the mean number of SCDs is 34 days per year. The largest SCDs are observed in

19   Northeast China at 167 days per year. Significant increases in SCDs are concentrated mainly in western

20   Northeast China (110°E - 128°E, 40°N - 50°N) from 1951 to 2018 (Figure 5b), and the proportion of

21   meteorological stations is 6.3% in total. The stations with significant decreases are distributed primarily

22   throughout central China, and the proportion is 9.3%. However, SCDs in the Tibetan Plateau tend to

23   decrease. Overall, the SCDs tend to increase at a rate of 0.5 days per decade from 1951 to 2018

24   throughout mainland China (Figure 6a); the SCDs first increase, then decrease and finally increase again,

25   and the changes appear in 1962 and 1986 (Figure 6b). Nevertheless, there are no significant trends in

26   SCDs throughout the study period.

27   In the three snow cover areas, the SCDs in Northeast China and northern Xinjiang both show

28   increasing trends, especially in Northeast China, where the increase is significant. The Tibetan Plateau

29   tends to decrease but not significantly, and the trends of the SCDs in Northeast China, northern Xinjiang

30   and the Tibetan Plateau are 2.3 days, 0.6 days and -0.5 days per decade, respectively (Table 4). The

31   overall break point of the SCDs in mainland China occurs in 1999. In Northeast China, the break points

32   of the SCDs occur in 1999. In northern Xinjiang, break points are observed in 1993 and 2002. In contrast,

33   there is no significant break point in the Tibetan Plateau. Furthermore, the distribution of the SCD trend
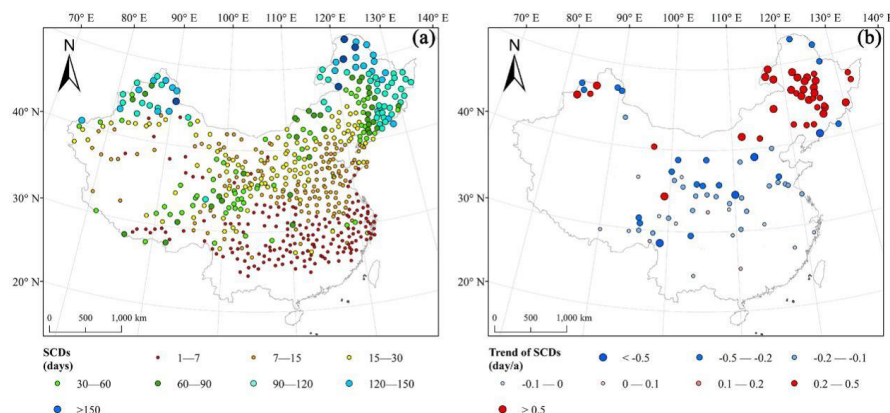
34   exhibits obvious regional differences.

Figure 5. Panel (a) presents the spatial distribution of the mean annual SCDs, and panel (b) displays the distribution of the mean annual trend of SCDs with significant changes ($P < 0.05$) as determined by trend analysis.
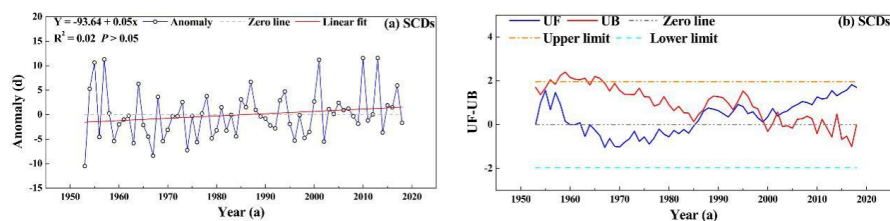

Figure 6. Panel (a) is the linear fit of the mean annual SCDs in China. Panel (b) presents the M-K test results for the mean annual SCDs in China.

Table 4. Trends in SCDs across the three snow cover areas from 1951 to 2018.

Zone	Slope analysis		M-K analysis
	Slope	P-value	Z-value
Northeast China	0.23	0.01**	2.46**
Northern Xinjiang	0.06	0.33	1.02
Tibetan Plateau	-0.05	0.16	-1.41

** denotes significance at < 0.01

4.3 Snow phenology

Figure 7 shows that the mean SDDs, SODs and SEDs are 99 days, 157th and 256th day, respectively. During the period from 1951 to 2018, the SDDs tend to shorten throughout mainland China, which is caused by the postponement of the SOD and the advance of the SED, and the trends of the SDDs, SOD and SED are -1.4 days, 0.4 days and -0.9 days per decade, respectively. The proportion of meteorological stations with significantly shortened SDDs is 25.2%, while the proportion of meteorological stations with a significant increasing trend in the SDDs is only 0.2%. The stations with significant delays in SOD are concentrated mainly in Northeast China, Northwest China and the Tibetan Plateau (Figure 7d), with a proportion among all meteorological stations of 14.3%. The stations with SODs that have become significantly earlier are mainly concentrated in Southeast China with a proportion of 2.8%. The stations with significant trends in the SED present mainly an advancing trend with a proportion of 17.6%, while the proportion of stations with a significant delay in the SED is only 0.3%. Table 5 shows that in Northeast
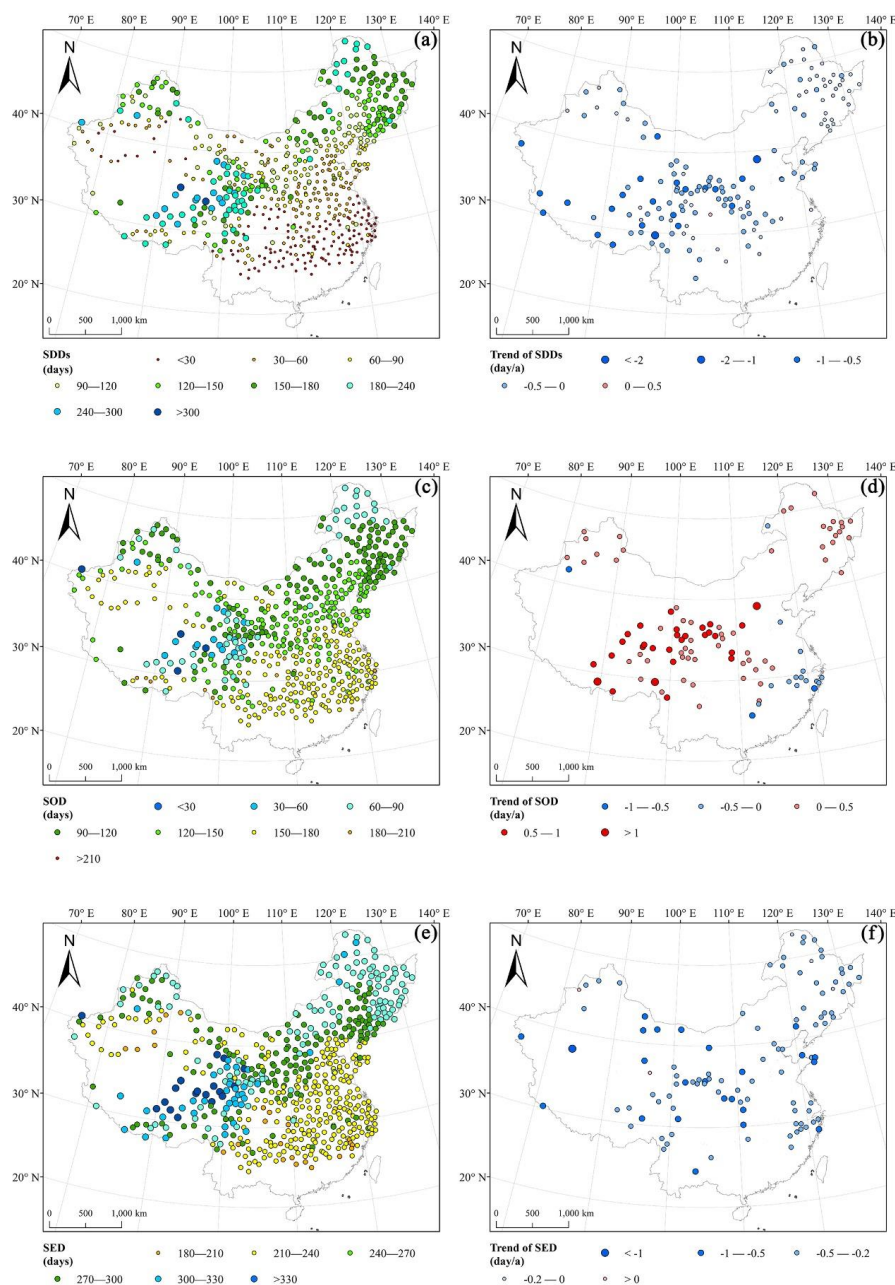
1   China, northern Xinjiang and the Tibetan Plateau, the reductions in SDDs reach 1.9 days, 1.0 days and

2   4.2 days per decade, respectively, the postponement of SOD is 0.5 days, 0.6 days and 3.3 days per decade,

3   and the advance of SED is 1.3 days, 0.4 days, and 0.8 days per decade, respectively.

4   **Table 5** Trends in snow phenology among the three snow areas from 1951 to 2018.

Zone	Variate	Slope analysis		M-K analysis
		Slope	*P*-value	Z-value
	SOD	0.05	0.34	0.91
Northeast	SED	-0.13	0.01**	-2.60**
	SDDs	-0.19	0.01**	-2.49**
	SOD	0.06	0.25	1.35
Northern Xinjiang	SED	-0.04	0.47	-1.11
	SDDs	-0.10	0.19	-1.51
	SOD	0.33	0.00**	4.88**
Tibetan Plateau	SED	-0.08	0.04*	-2.14*
	SDDs	-0.42	0.00**	-4.51**

5   ** denotes a significant change at P < 0.05.

6

1
2 **Figure 7.** Panels (a), (c) and (e) present the spatial distributions of the mean annual SDDs, the mean
3 annual SOD and the mean SED across China, respectively. Panels (b), (d) and (f) display the distributions
4 of the trend of the mean annual SDDs, the mean annual SOD and the mean SED with significant changes
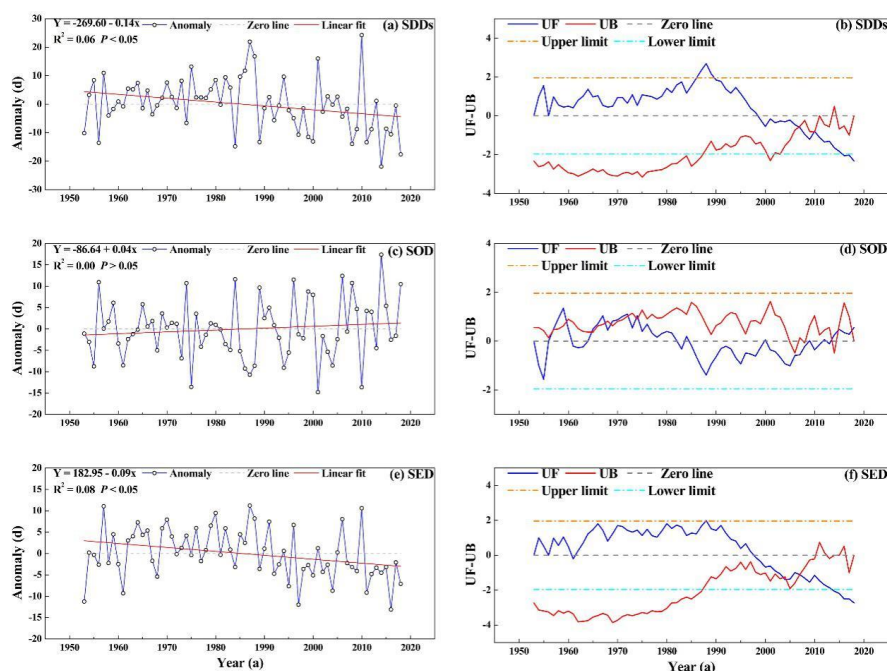5 ($P < 0.05$) across China as determined by trend analysis.

Figure 8. Panels (a), (c) and (e) present the linear fits of the mean annual SDDs, the mean annual SOD and the mean SED in China, respectively. Panels (b), (d) and (f) present the M-K test results of the mean annual SDDs, the mean annual SOD and the mean SED in China, respectively.
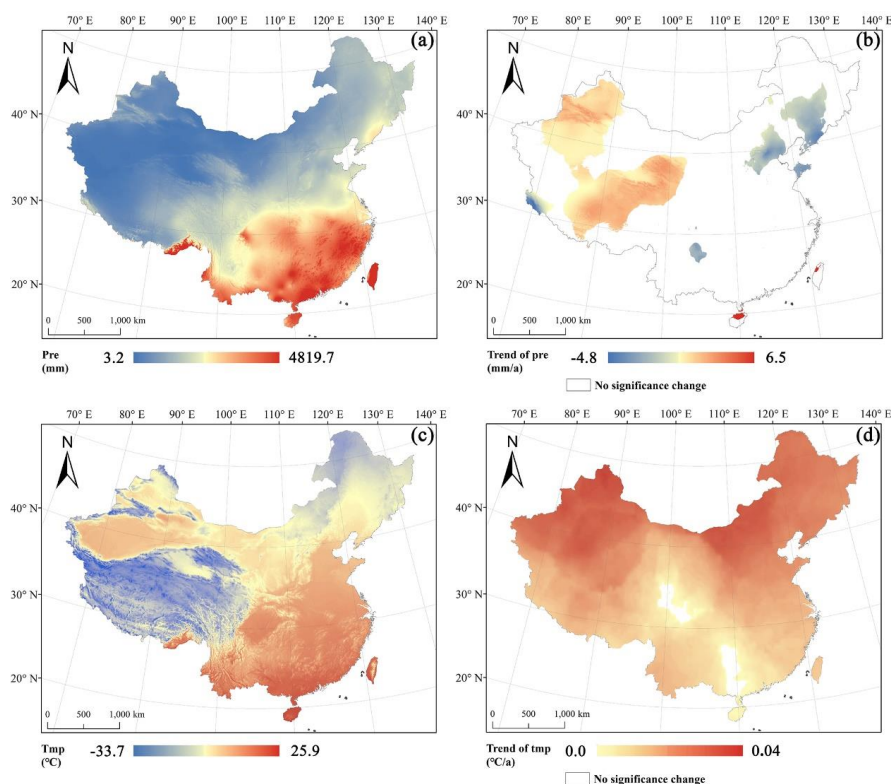
Figure 8 indicates that the SDDs first increase and then decrease, and the trend transforms in 1999, and significant increases occur from 1987 to 1989. The trend of the SOD changes many times, showing an upward trend from 1964 to 1982, followed by a downward trend from 1985 to 2013. The SED tends to delay at first and then appears earlier, and the trend transforms in 1998. The break point of SDDs occurs in 2005, the SOD break points appear in 1959 and 1964, and the SED break point is observed in 2004. The spatiotemporal variations in snow cover phenology show obvious regional heterogeneity. In Northeast China, the break point of SDDs occurs in 2000, the SOD break point appears in 2005, and the SOD break point is observed in 2001. In northern Xinjiang, the break points of the SDDs are observed in 1999 and 2001, the SOD break point occurs in 1970, and the SED break point appears in 1996. In the Tibetan Plateau, the break point of the SDDs is in 2005, the SOD break point occurs in 2001, and the SED break point appears in 2009. Overall, from 1951 to 2018 in mainland China, the SDDs, SOD and SED are highly related to geographical zonality, and their trends are shortened, delayed and appear earlier, respectively. The main reason for the shortening of SDDs is the SED appearing earlier. However, in the Tibetan Plateau, the main reason for the shortened SDDs is the delay in SOD. Furthermore, the snow phenology changes in the Tibetan Plateau are greater than those elsewhere.

4.4 Snow heterogeneity

Figure 9 shows that the trend of annual precipitation shows that the significantly increasing trend is mainly concentrated in western China from 1953 to 2017, especially in Xinjiang and the inner Tibetan Plateau. However, the significantly decreasing trend of precipitation is mainly concentrated in Northeast China. The proportions of the areas with significantly increasing trends and decreasing trends are 20.4% and 6.8%, respectively. The annual mean temperature tends to increase throughout China from 1953 to

1   2017. In addition, up to 97.2% of the region showed a significantly increasing trend, with a maximum
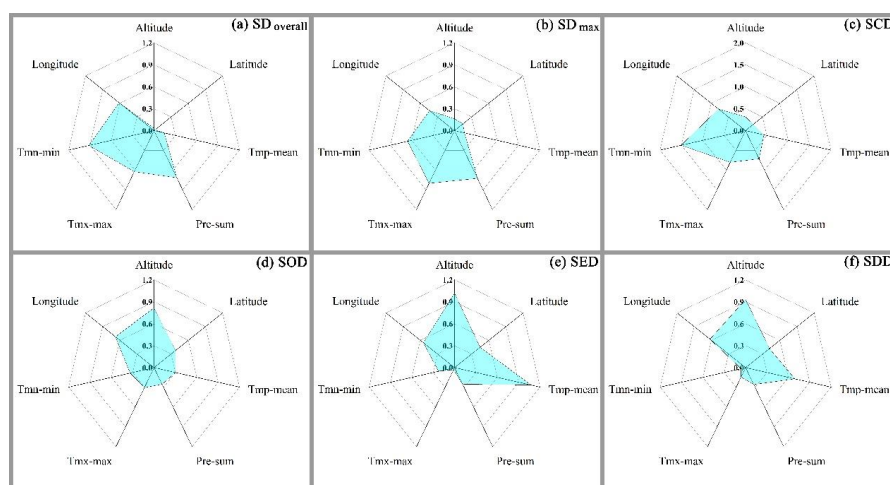
2   trend of 0.04 °C per year.

3

4   **Figure 9.** Panels (a) and (c) represent the annual mean precipitation and temperature, and panels (b) and

5   (d) are the significant trends ($P < 0.05$) from 1951-2017 across China.

6   Figure 10 indicates that the geographical and meteorological factors all affect SD, SCDs and snow

7   phonology indirectly and directly. Longitude, temperature and precipitation have an impact on $SD_{overall}$,

8   while latitude and altitude do not impact $SD_{overall}$, of which the maximum total standardized effect is the

9   annual coldest monthly minimum temperature (Tmn-min), with a coefficient up to 0.9. All factors affect

10   the spatial and temporal distribution of SD_{max}, and interestingly, the annual warmest monthly maximum

11   temperature (Tmx-max) is the most important factor controlling the SD_{max}, and the coefficient of the total

12   standardized effect is 0.8. This factor was followed by the annual total precipitation (Pre-sum), Tmn-min

13   and longitude. The SCD distribution is also controlled by all geographical and meteorological factors, of

14   which the Tmn-min is the most important factor with a total standardized effect of 1.5. The geographical

15   and meteorological factors have an impact on the SOD, but the altitude is the most sensitive to the start

16   time of snow cover. The higher the altitude is, the earlier SOD is. The most important factor that controls

17   SED is the annual mean temperature (Tmp-mean), with the largest total standardized effect coefficient

18   of 1.1. Altitude is another important factor affecting SED. However, SCDs include only empirical

19   ephemeral snow days compared to SDDs, and the contributions to SCDs and SDDs are completely

20   inconsistent. Although Tmn-min is the most important factor controlling the SCD distribution, its effect

14

1 on SDDs is negligible. Altitude has the largest total standardized effect coefficient of 0.9, which has the

2 most important effect on SDDs, followed by Tmp-mean, longitude and latitude.

4 **Figure 10.** Panels (a-g) show the standardized total effects of geographic and meteorological factors on

5 snow cover parameters, including the $SD_{overall}$, SD_{max}, SCDs, SOD, SDDs, and SED.

6 **5   Discussion**

7 The variation and distribution of snow cover and its causes have always been a popular topic. In this

8 study, snow indices calculated based on data from meteorological stations over the past 60 years were

9 analyzed in China. The overall SCDs in China are increasing, the SOD is delayed, the SED has been

10 appearing earlier, and the SDDs are shortened. Nevertheless, the SD shows an increasing trend, especially

11 in Northeast China. The snow parameters show different oscillatory periods also found in this study

12 between 1951 and 2018.

13   Regarding the SD, using passive microwave remote sensing, Che et al. (2008) found that the SD in

14 China showed a weak increasing trend from 1978 to 2006. Zhong et al. (2018) found that both the annual

15 mean and the maximum SD showed increasing trends over the entire Eurasian continent, including China,

16 and the snow depth decreased in autumn and increased in spring and winter. The results of our study are

17 roughly the same as those of this previous study. The areas where $SD_{overall}$ and SD_{max} increased

18 significantly were mainly concentrated at latitudes above 40 °N. The results of both the M-K analysis

19 and slope methods show similar changes in Northeast China and northern Xinjiang. Huang et al. (2016)

20 also found a significant increasing trend of SD in Northeast China, whereas SD decreased in the north

21 and northwest regions of the Tibetan Plateau from 2000 to 2014 according to MODIS snow products.

22 This study also found decreasing trends of $SD_{overall}$ and SD_{max} from 1951 to 2018 in the Tibetan Plateau.

23 Wei & Dong (2015) used the results of CMIP5 multimodel averages to assess and simulate the SD in the

24 Tibetan Plateau, and they found that SD indicated decreases for most of the models from 1851 to 2005.

25 However, the results from CMIP5 overestimated snow depth over the Tibetan Plateau.

26   The SCDs at the middle and low latitudes of the Northern Hemisphere, including Northeast China,

27 showed an increasing trend from 2000 to 2015 according to the MODIS snow cover dataset (Huang et

28 al. 2016; Wang et al. 2018). A large number of studies have also found that the SCDs on the Tibetan

29 Plateau show a declining trend (Chen et al., 2015; Huang et al., 2017; Qiao et al., 2018). Hori et al. (2017)

30 found regional differences in the SCD changes among the three stable snow cover areas in China by

using long-term JASMES (JAXA Satellite Monitoring for Environmental Studies) snow cover products. However, our study obtains similar results by using a dataset from meteorological stations. In our study, we found that the SCDs increased in Northeast China, northern Xinjiang and even throughout China. However, the SCDs of the Tibetan Plateau shortened from 1951 to 2018. This result is also similar to the results obtained by Huang et al. (2017), who used MODIS daily snow cover products from 2001 to 2014.

Regarding snow phenology, Ke et al. (2016) found that from 1952 to 2010, the overall snow phenology in China reflected a delay of the SOD and an advancement of the SED. Peng et al. (2017) found that compared to the entire Northern Hemisphere, there was a significant increase in the SEDs that appeared earlier among the three stable snow cover areas in China from 1979 to 2006. This result is similar to the results of our study. The snow phenology indicated a shortened number of SDDs, a delay in the SOD and an advancement in the SED in China; among them, the SDDs and the SED changed significantly from 1951 to 2018. In Northeast China, the trends of SOD, SED and SDDs are similar to those in China. In particular, the SED has been appearing earlier and contributes more to the reduction in SDDs. However, in the Tibetan Plateau, the trends of SOD, SED and SDDs are all significant. The trend of SOD (0.3 days per year) is much larger than that of SED (-0.1 days per year). Therefore, the main reason for the shortening of the SDDs in the Tibetan Plateau may be the significant delay of the SOD. Using a combination of these six snow cover indices, we found that the $SD_{overall}$ and SD_{max} in China increased, especially in Northeast China and northern Xinjiang, from 1951 to 2018. However, the $SD_{overall}$ and SD_{max} on the Tibetan Plateau showed a weakly decreasing trend. In summary, more SCDs and shorter SDDs led to increased snow cover across China from 1951 to 2018.

In mainland China, the distribution of snow cover exhibits strong zonality, and the snow depth and its phenology are highly spatially and temporally heterogeneous. A large number of studies have proven that meteorological and geographic factors are closely related to snow cover (Ye, 2018; Zhong, 2018). However, geographical factors are a direct factor that affects climate and indirectly affects snow cover distribution. Therefore, meteorological factors, including temperature and precipitation, are very important factors affecting snow cover. This study shows that meteorological factors not only affect the depth of snow cover but also have an important influence on the phenology of snow cover; in particular, the influence of the temperature effect on snow is obvious. With climate change, especially climate warming, snow depth and its phenology will change severely, which will dominate the rise in temperature in the future.

6 Conclusion

The variation and distribution of snow cover have always been popular research topics. Here, we assessed snow cover variations using in situ observations provided by the CMA across mainland China from 1951 to 2018. The conclusions of this study are as follows:

1) Snow depth tends to increase in China, of which the overall $SD_{overall}$ and SD_{max} tend to increase significantly in Northeast China, and nonsignificantly in northern Xinjiang. However, $SD_{overall}$ and SD_{max} both show decreasing trends in the Tibetan Plateau, but the trend is negligible.

2) SCDs in Northeast China and northern Xinjiang both show increasing trends, especially in Northeast China, where the increase is significant. However, the SCDs in the Tibetan Plateau tend to decrease but not significantly.

3) SDDs tend to shorten throughout mainland China, which is caused by the SOD delay, and the SED has been appearing earlier. Furthermore, the snow phenology changes in the Tibetan Plateau are greater than those elsewhere.

4) Geographical and meteorological factors are the main factors controlling the heterogeneity of the spatial distribution of snow depth and phenology, while changes in meteorological factors have a more important influence on snow cover distribution, especially changes in temperature, which will lead to significant changes in snow depth and phenology.

Author contribution. X.D. Huang conceived the research and wrote the paper. T.G. Liang and Z.J. Zheng guided the implementation of the research, and revised and finalized the manuscript. C.Y. Liu provided data analysis and graphic drafting. Y.L. Wang provided the data analysis and suggestions.

Competing interests. The authors declare no conflicts of interest.

References

Ambadan, J. T., and Berg, A. A., Merryfield, W. J., and Lee W.: Influence of snowmelt on soil moisture and on near surface air temperature during winter–spring transition season, Clim. Dynam., 51, 1-15, http://doi.org/10.1007/s00382-017-3955-8, 2017.

Armstrong, R. L., and Brodzik, M. J.: Recent Northern Hemisphere Snow Extent, A Comparison of Data Derived from Visible and Microwave Satellite Sensors, Geophys. Res. Lett., 28, 3673-3676, http://doi.org/10.1029/2000gl012556, 2001.

Bagozzi, R. P., and Yi, Y.: Specification, evaluation, and interpretation of structural equation models, J. Acad. Market. Sci., 40, 8-34, http://doi.org/10.1007/s11747-011-0278-x, 2012.

Brown, R. D., Robinson, D. A., 2011. Northern Hemisphere spring snow cover variability and change over 1922–2010 including an assessment of uncertainty. Cryosphere. 5, 219–229.

Che, T., Xin, L., Jin, R., Armstrong, R., and Zhang, T.: Snow depth derived from passive microwave remote-sensing data in China, Ann. Glaciol., 49, 145-154, http://doi.org/10.3189/172756408787814690, 2008.

Chen, W., Ding, J., Sun, Y., Wang, J., and Zhang, Z.: Retrieval of snow cover area based on NDSI-NDVI feature space, J. Galciol. Geocryol., 37, 1059-1066, http://doi.org/10.7522/j.issn.1000-0240.2015.0118, 2015.

Chen, X., Liang, S., Cao, Y., He, T.: Distribution, attribution, and radiative forcing of snow cover changes over China from 1982 to 2013. Clim. Change. 137, 363–77, 2016.

Choi, G., Robinson, D., and Kang, S.: Changing Northern Hemisphere snow seasons. J. Clim. 23, 5305–5310, 2010.

Cohen, J., Furtado, J., Jones, J., Barlow, M., Whittleson, D., and Enekhabi, D.: Linking Siberian snow cover to precursors of stratospheric variability, J. Clim., 27, 5422-5432, 2014.

Connolly, R., Connolly, M., Soon, W., Legates, D. R., Cionco, R. G., Velasco Herrera, V. M.: Northern Hemisphere snow-cover trends (1967-2018): A comparison between climate models and observations. Geosci. 9, 030135, 2019.

Derksen, C., Brown, R.: Spring snow cover extent reductions in the 2008-2012 period exceeding climate

The Cryosphere
Discussions

1 model projections. Geophys. Res. Lett. 39, 053387, 2012.

2 Dyer, J. L. and Mote, T.: Spatial variability and trends in observed snow depth over North America,
3   Geophys. Res. Lett., 33, L16503, 2006.

4 Euskirchen, E. S., McGuire, A. D., Chapin, F.S.: Energy feedbacks of northern high-latitude ecosystems
5   to the climate system due to reduced snow cover during 20th century warming. Glob. Chang. Biol.
6   13, 2425–2438, https://doi.org/10.1111/j.1365-2486.2007.01450.x, 2007.

7 Grace, J.B., Anderson, T.M., Olff, H., Scheiner, S.M.: On the specification of structural equation models
8   for ecological systems. Ecol. Monogr. 80, 67–87. https://doi.org/10.1890/09-0464.1, 2010.

9 Grace, J.B., Anderson, T.M., Seabloom, E.W., Borer, E.T., Adler, P.B., Harpole, W.S., Hautier, Y.,
10   Hillebrand, H., Lind, E.M., Pärtel, M., Bakker, J.D., Buckley, Y.M., Crawley, M.J., Damschen, E.I.,
11   Davies, K.F., Fay, P.A., Firn, J., Gruner, D.S., Hector, A., Knops, J.M.H., MacDougall, A.S.,
12   Melbourne, B.A., Morgan, J.W., Orrock, J.L., Prober, S.M., Smith, M.D.: Integrative modelling
13   reveals mechanisms linking productivity and plant species richness. Nature 529, 390–393.
14   https://doi.org/10. 1038/nature16524, 2016.

15 Hall, D.K., Riggs, G.A., Salomonson, V.V., DiGirolamo, N.E., Bayr, K.J.: MODIS snow-cover products.
16   Remote Sens. Environ. 83, 181–194, 2002.

17 Hori, M., Sugiura, K., Kobayashi, K., Aoki, T., Tanikawa, T., Kuchiki, K., Niwano, M., Enomoto, H.: A
18   38-year (1978–2015) Northern Hemisphere daily snow cover extent product derived using
19   consistent objective criteria from satellite-borne optical sensors, Remote. Sens. Environ., 191, 402-
20   418, 2017.

21 Huang X., Deng, L., Ma, X., Wang Y., Hao, X., and Liang, T.: Spatiotemporal dynamics of snow cover
22   based on multi-source remote sensing data in China, Cryosphere, 10, 2453-2463,
23   http://doi.org/10.5194/tc-10-2453-2016, 2016.

24 Huang, X., Deng, J., Wang, W., Feng, Q., and Liang, T.: Impact of climate and elevation on snow cover
25   using integrated remote sensing snow products in Tibetan Plateau, Remote. Sens. Environ., 190,
26   274-288, http://doi.org/10.1016/j.rse.2016.12.028, 2017.

27 Ke, C., Li, X., Xie, H. Liu, X., and Kou, C.: Variability in snow cover phenology in China from 1952 to
28   2010, Hydrol. Earth Syst. Sc., 20, 755-770, http://doi.org/10.5194/hess-20-755-2016, 2016.

29 Kitaev, L., Førland, E., Razuvaev, V., Tveito, O. E., and Krueger, O.: Distribution of snow cover
30   over Northern Eurasia, Nord. Hydrol., 36, 311-319, 2005.

31 Li, L., and Simonovic, S. P.: System dynamics model for predicting floods from snowmelt in North
32   American prairie watersheds, Hydrol. Process., 16, 2645-2666, http://doi.org/10.1002/hyp.1064,
33   2010.

34 Listion, G.E., and Hiemstra, C.A.: The changing cryosphere: Pan-Arctic snow trends (1979-2009),
35   J. Climate, 24, 5691-5712, 2011.

36 Ma, L., Qin, D., Bian, L., Xiao, C., and Lou, Y.: Sensitivity of the Number of Snow Cover Days to
37   Surface Air Temperature over the Qinghai-Tibetan Plateau, Adv. Clim. Change Res., 2010, 76-83,
38   http://doi.org/10.3724/SP.J.0000.2010.00076, 2010.

39 Milan, G., and Slavisa, T.: Analysis of changes in meteorological variables using Mann-Kendall and
40   Sen's slope estimator statistical tests in Serbia, Global Planet Change, 100, 172-182,
41   http://doi.org/10.1016/j.gloplacha.2012.10.014, 2013.

42 Mudryk, L., M. Santolaria-Otín, Krinner, G., Ménégoz, M., Derksen, C., Brutel-Vuilmet, C., Brady,
43   M., Essery, R: Historical Northern Hemisphere snow cover trends and projected changes in the
44   CMIP-6 multi-model ensemble, The Cryosphere. 14, 2495–2514, http://doi.org/10.5194/tc-14-

The Cryosphere
Discussions

Open Access

EGU

1   2495, 2020.

2   Peng, S., Piao, S., Ciais, P., Friedlingstein, P., Zhou, L., Wang, T.: Change in snow phenology and its
3   potential feedback to temperature in the Northern Hemisphere over the last three decades, Environ.
4   Res. Letters., 8, 014008, 2013.

5   Pulliainen, J.: Mapping of snow water equivalent and snow depth in boreal and sub-arctic zones by
6   assimilating space-borne microwave radiometer data and ground-based observations. Remote Sens.
7   Environ. 101, 257–269, 2006.

8   Pulliainen, J., Luojus, K., Derksen, C., Mudryk, L., Lemmetyinen, J., Salminen, M., Ikonen, J.,
9   Takala, M., Cohen, J., Smolander, T., & Norberg, J.: Patterns and trends of Northern
10   Hemisphere snow mass from 1980 to 2018. Nature, 581(7808), 294–298.
11   https://doi.org/10.1038/s41586-020-2258-0, 2020.

12   Qiao, D., Wang, N., Li, Z., Zhou, J., and Fu, X.: Spatio-temporal changes of snow phenology in the
13   Qinghai-Tibetan Plateau during the hydrological year of 1980-2009, Clim. Change Res., 14, 137-
14   143. http://doi.org/10.12006/j.issn.1673-1719.2017.088, 2018.

15   Shams, M. S., Faisal Anwar, A. H. M., Lamb, K. W., and Bari, M.: Relating ocean-atmospheric climate
16   indices with Australian river streamflow, J. Hydrol., 556, 294-309,
17   http://doi.org/10.1016/j.jhydrol.2017.11.017, 2018.

18   Sönmez, I., Tekeli, A.E., Erdi, E.: Snow cover tendency analysis using Interactive Multisensor Snow and
19   Ice Mapping System data over Turkey. Int. J. Climatol. 34, 2349–2361, 2014.

20   Soon, W. H., Connolly, R., Connolly, M., O'Neill, P., Zheng, J., Ge, Q., Hao, Z., Yan, H.: Comparing the
21   current and early 20th century warm periods in China, Earth-Sci. Rev., 185, 80-101, 2018.

22   Stow, D.A., Hope, A., McGuire, D., Verbyla, D., Gamon, J., Huemmrich, F., Houston, S., Racine,
23   C., Sturm, M., Tape, K., et al.: Remote sensing of vegetation and land-cover change in Arctic
24   Tundra Ecosystems. Remote Sens. Environ. 89, 281–308, 2004.

25   Sun, Y, Zhang, T, Liu, Y, Zhao, W., Huang, X.: Assessing snow phenology over the large part of
26   Eurasia using satellite observations from 2000 to 2016, Remote Sens. 12, 2060,
27   http://doi.org/10.3390/rs12122060, 2020.

28   Takala, M., Luojus, K., Pulliainen, J., Derksen, C., Lemmetyinen, J., Kärnä, J.P., Koskinen, J., Bojkov
29   B.: Estimating northern hemisphere snow water equivalent for climate research through assimilation
30   of space-borne radiometer data and ground-based measurements. Remote Sens. Environ. 115, 3517–
31   3529, 2011.

32   Tedesco, M., Miller, J.: Observations and statistical analysis of combined active–passive microwave
33   space-borne data and snow depth at large spatial scales. Remote sens. Environ. 111, 382-397, 2007.

34   Wang, Y., Huang, X., Liang, H., Sun, Y., Feng, Q., and Liang, T.: Tracking Snow Variations in the
35   Northern Hemisphere Using Multi-Source Remote Sensing Data (2000–2015), Remote Sensing, 10,
36   136, http://doi.org/10.3390/rs10010136, 2018.

37   Wei, Z., and Dong, W.: Assessment of Simulations of Snow Depth in the Qinghai-Tibetan Plateau Using
38   CMIP5 Multi-Models, Arctic Antarct. & Alp. Res., 47, 611-525, 2015.

39   Xiao, L., and Che, T.: Preliminary Study on Snow Feedback to the Climate System in the Tibetan Plateau,
40   Remot. Sens. Technol. Appl., 30, 1066-1075, http://doi.org/10.11873/j.issn.1004-0323.2015.6.1066,
41   2016.

42   Yao, T., Qin, D., Shen, Y., Zhao, L., Wang, N., and Lu, A.: Cryospheric changes and their impacts on
43   regional water cycle and ecological conditions in the Qinghai Tibetan Plateau, Chin. J. Nat., 35,
44   179-186, http://doi.org/10.3969/j.issn.0253-9608.2013.03.004, 2013.

The Cryosphere
Discussions

Open Access

EGU

1   Ye, K.: Interannual variability of March snow mass over Northern Eurasia and its relation to the
2   concurrent and preceding surface air temperature, precipitation and atmospheric circulation, Clim.
3   Dyn. 10.1007/s00382-018-4297-x, 2018.
4   Zhong, X., Zhang, T., Zheng, L., Hu, Y., Wang, H., and Kang, S.: Spatiotemporal variability of snow
5   depth   across   the   Eurasian   continent   from   1966   to   2012,   Cryosphere,   12,   227-245,
6   https://doi.org/10.5194/tc-12-227-2018, 2018.